Atmos. Chem. Phys. Discuss., https://doi.org/10.5194/acp-2017-1074
Manuscript under review for journal Atmos. Chem. Phys.
Discussion started: 28 November 2017

Atmospheric Chemistry and Physics Discussions

The influence of model spatial resolution on simulated ozone and fine particulate matter: implications for health impact assessments

Sara Fenech[1,2], Ruth M. Doherty[1], Clare Heaviside[2], Sotiris Vardoulakis[3], Helen L. Macintyre[2], Fiona M. O'Connor[4]

[1] School of GeoSciences, University of Edinburgh

[2] Centre for Radiation, Chemical and Environmental Hazards, Public Health England

[3] Institute of Occupational Medicine

[4] Met Office, Hadley Centre, Exeter, UK

Correspondence to: Sara Fenech (S.Fenech@sms.ed.ac.uk)

Abstract. We examine the impact of model horizontal resolution on simulated surface ozone (O_3) and particulate matter less than 2.5 μm ($PM_{2.5}$) concentrations, and the associated health impacts over Europe, using the HadGEM3-UKCA chemistry-climate model to simulate pollutant concentrations over Europe at a global (~ 140 km) and a regional (~ 50 km) resolution. The attributable fraction (AF) of total mortality due to long-term exposure to warm season daily maximum 8-hour running mean (MDA8) O_3 and annual-average $PM_{2.5}$ concentrations is then calculated for each European country using pollutant concentrations simulated at each resolution. Our results highlight a strong seasonal variation in simulated O_3 and $PM_{2.5}$ differences between the two model resolutions in Europe. Compared to the regional resolution results, simulated European O_3 concentrations at the global resolution are on average higher in winter and spring (10% and 6%, respectively). In contrast, simulated O_3 concentrations at the global resolution are lower in summer and autumn (-1% and -4%, respectively). These differences may partly be explained by differences in nitrogen dioxide (NO_2) concentrations simulated at the two resolutions. Compared to O_3, we find the opposite seasonality in simulated $PM_{2.5}$ differences between the two resolutions. In winter and spring, simulated $PM_{2.5}$ concentrations are lower at the global compared to the regional resolution (-8% and -27%, respectively) but higher in summer and autumn (29% and 8%, respectively) and are mostly related to differences in convective rainfall between the two resolutions for all seasons. These differences between the two resolutions exhibit clear spatial patterns for both pollutants that vary by season, and exert a strong influence on country to country variations in estimated AF for the two resolutions. Warm season MDA8 O_3 levels are higher in most of southern Europe, but lower in areas of northern and eastern Europe when simulated at the global resolution compared to the regional resolution. Annual-average $PM_{2.5}$ concentrations are higher across most of northern and eastern Europe but lower over parts of southwest Europe at the global compared to the regional resolution. Across Europe, differences in the AF associated with long-term exposure to population-weighted MDA8 O_3 range between -0.9 % and +2.6 % (largest positive differences in southern Europe) while differences in the AF associated with long-term exposure to population-weighted annual mean $PM_{2.5}$ range from -4.7% to +2.8% (largest positive differences

Atmos. Chem. Phys. Discuss., https://doi.org/10.5194/acp-2017-1074
Manuscript under review for journal Atmos. Chem. Phys.
Discussion started: 28 November 2017

in eastern Europe) of the total mortality. Therefore this study, with its unique focus on Europe, demonstrates that health impact assessments calculated using modelled pollutant concentrations, are sensitive to a change in model resolution by up to ±5% of the total mortality across Europe.

1 Introduction

A substantial number of epidemiological studies have derived risk estimates for mortality associated with long-term exposure to ambient fine particulate matter with aerodynamic diameter less than 2.5 µm ($PM_{2.5}$) (Krewski, 2009;Brook et al., 2010; WHO, 2013) and also recently, to a lesser extent, for long-term exposure to ozone (O_3) (Jerrett et al., 2009; Forouzanfar et al., 2016; Turner et al., 2016). Differences in risk estimates produced from different epidemiological studies can be due to differences in methodologies, air pollution and health data used including the size and spatial extent of cohort populations. For O_3, these long-term risk estimates are derived from North American studies. In this region O_3 data is typically monitored only during the O_3 season (April-September), hence these derived O_3-risk estimates apply only to the ozone occurring in the warm season part of the year.

Air pollutant exposure estimated from concentrations measured at fixed monitoring stations, is often used to estimate health impacts at the cohort-scale (Cohen et al., 2004). However, quantifying the adverse health effects of air pollution at the continental-scale requires global or regional atmospheric models (with resolutions ranging from ~250 to 50 km) to simulate pollutant spatio-temporal distributions across these scales (e.g. West et al. 2009; Anenberg et al. 2010; Fang et al. 2013; Silva et al. 2013; Lelieveld et al. 2015). Amongst a number of factors, simulated air pollutant concentrations may vary depending on the three-dimensional chemistry model used, its set-up and the model resolution (e.g. Markakis et al. 2015; Schaap et al. 2015; Yu et al. 2016; Neal et al. 2017). Although the same model processes are represented at different model resolutions, simulated pollutant concentrations can vary due to differences in (i) the resolution of emissions, which may have a nonlinear effect on the chemical formation of pollutants, and (ii) the driving meteorology (Valari and Menut 2008; Tie et al. 2010; Arunachalam et al. 2011; Colette et al. 2013; Markakis et al. 2015; Schaap et al. 2015).

The impact of model horizontal resolution on simulated O_3 concentrations has been primarily linked to less dilution of emissions when using fine resolutions (Valari and Menut 2008; Tie et al. 2010; Colette et al. 2013; Stock et al. 2014; Schaap et al. 2015). Investigating the impact of increasing model horizontal resolution from 48 km to 6 km on O_3 concentrations in Paris, Valari and Menut (2008) found modelled surface O_3 to be more sensitive to the resolution of input emissions than to meteorology. A number of other studies note the sensitivity of simulated O_3 to simulated nitrogen oxide (NO_x) concentrations that determine the extent of titration of O_3 by nitrogen monoxide (NO) (Stock et al., 2014; Markakis et al., 2015; Schaap et al., 2015). Stock et al. (2014) further found the impact of spatial resolution (150km vs. 40km) on simulated O_3 concentrations to vary with season across Europe. In winter, higher NO_x concentrations produced more pronounced titration effects on O_3 at 40 km resolution, leading to lower O_3 concentrations than at 150 km resolution. In summer, the simulated boundary layer height was suggested to be largely responsible for the differences in O_3 concentrations at the two resolutions.

$PM_{2.5}$ concentrations have also been found to be sensitive to the model horizontal resolution (Arunachalam et al. 2011; Punger and West 2013; Markakis et al. 2015; Neal et al. 2017). In the U.S., Punger and West (2013) found population-weighted annual mean $PM_{2.5}$ concentrations to be 6% higher at 36 km compared to 12 km, but 27% lower when simulated at 408 km compared to 12 km. However in this study, statistical averaging was used to estimate pollutant concentrations at the coarsest resolutions, and therefore differences in emissions and meteorology and their atmospheric processing between the resolutions were not included. In contrast, Li et al. (2016) found annual mean $PM_{2.5}$ concentrations simulated at a resolution of ~ 2.5° in the U.S. to be similar to $PM_{2.5}$ concentrations simulated at a resolution of ~ 0.5° suggesting that the horizontal scales being compared and the methodology for comparison are important. However maximum $PM_{2.5}$ concentrations which occur in highly populated regions were found to be 21% lower at the coarse resolution (Li et al., 2016).

As outlined above, a number of studies have analysed the effect of model resolution on O_3 and $PM_{2.5}$ concentrations but few have looked at the sensitivity of the associated health impacts to model resolution (Punger and West 2013; Thompson et al. 2014; Li et al. 2015). Punger and West (2013) found mortality associated with long-term exposure to O_3 in the US to be 12% higher at a 36 km resolution compared to the mortality estimate at 12 km, as a result of higher O_3 simulated at the coarser-scale. For $PM_{2.5}$-related health estimates, studies by Punger and West (2013) and Li et al. (2016) both found that attributable mortality associated with long-term exposure to $PM_{2.5}$ in the US was lower for their coarser resolution simulations (> 100 km) due to lower simulated $PM_{2.5}$ concentrations in densely populated regions. However, Thompson et al. (2014) found that using model horizontal resolutions of 36, 12 and 4 km had a negligible effect on changes in $PM_{2.5}$ concentrations and associated health impacts. This is likely due to the relatively small range of resolutions used by Thompson et al. (2014) compared to these other studies.

The majority of health effect studies relating to the impact of model resolution have been conducted in North America. Hence, similar studies are lacking over Europe. This study is therefore the first to examine the impact of two different model resolutions: a global (~ 140 km) and regional resolution (~ 50 km) on O_3 and $PM_{2.5}$ concentrations, and their subsequent impacts on European-scale human health through long-term exposure to O_3 and $PM_{2.5}$. We define the sensitivity of health impacts to model resolution by calculating the attributable fraction (AF) of total mortality which is associated with long-term exposure to O_3 and $PM_{2.5}$ for various European countries, based on simulated concentrations at both resolutions, and expressed as a percentage.

The remainder of the paper is organised as follows. Section 2 describes the modelling framework used for both the global and regional simulations and the methods used to calculate the AF of mortality associated with O_3 and $PM_{2.5}$ for various European countries. Section 3 presents differences in seasonal mean O_3 and $PM_{2.5}$ concentrations between the two resolutions. In section 4, we first analyse differences in warm season daily maximum 8-hour running mean (MDA8) O_3 concentrations and annual $PM_{2.5}$ concentrations between the two resolutions, then quantify differences in country-level population-weighted MDA8 O_3 and annual mean $PM_{2.5}$ concentrations. Secondly, the country-level AF associated with long-term exposure to MDA8 O_3 and annual mean $PM_{2.5}$ simulated at both resolutions are presented. The conclusions of this study are then presented in Section 5.

Atmos. Chem. Phys. Discuss., https://doi.org/10.5194/acp-2017-1074
Manuscript under review for journal Atmos. Chem. Phys.
Discussion started: 28 November 2017

2 Methods

2.1 Model description and experimental setup

The two configurations used in this study are based on the Global Atmosphere 3.0 (GA3.0) / Global Land (GL3.0) configuration of the Hadley Centre Global Environmental Model version 3 (HadGEM3, Walters et al., 2011), of the Met Office's Unified Model (MetUM, Brown et al., 2012). The global configuration has a horizontal resolution of 1.875° × 1.25° (~ 140 km, Walters et al., 2011) while the regional configuration has a horizontal resolution of 0.44° × 0.44° (~50 km, Moufouma-Okia and Jones, 2014) with a domain covering most of Europe.

As this study focuses on health impacts, our analysis is restricted to European land regions. In both configurations, a 63 level hybrid height vertical co-ordinate system is used with 50 levels below 18 km and a surface level at 40 m. Gas phase chemistry is simulated within HadGEM3 by a tropospheric configuration of the United Kingdom Chemistry and Aerosol (UKCA) model (Morgenstern et al., 2009; O'Connor et al., 2014). The chemistry scheme used for both configurations is the UKCA Extended Tropospheric Chemistry (UKCA-ExtTC) scheme (Folberth et al., In prep.) which is an extension to the TropIsop standard chemistry scheme (O'Connor et al., 2014) and includes 89 chemical species. Boundary layer mixing for both configurations is based on Lock et al. (2000) and includes an explicit entrainment parametrisation and non-local mixing in unstable layers. The GA3.0/GL3.0 configuration of HadGEM3 (Walters et al., 2011) also includes an interactive aerosol scheme called CLASSIC (Coupled Large-scale Aerosol Simulator for Studies in Climate; Jones et al., 2001;Bellouin et al., 2011) from which $PM_{2.5}$ concentrations are estimated. CLASSIC simulates ammonium sulphate and nitrate, fossil-fuel organic carbon (FFOC), mineral dust, soot and biomass burning (BB) aerosol interactively. Biogenic secondary organic aerosols are prescribed from a climatology. Sea salt aerosol is diagnosed over ocean only and does not contribute to particulate matter over land.

The model simulations for both these configurations cover a period of one year and 9 months starting from April 2006, from which the first nine months were discarded as spin-up. The global configuration uses monthly mean distributions of sea surface temperature (SST) and sea ice cover (SIC), derived for the present-day (1995-2005) from transient coupled atmosphere-ocean simulations (Jones et al., 2001) of the HadGEM2-ES model (Collins et al., 2011). Using a simple linear re-gridding algorithm, the SST and SIC climatologies developed for the global configuration were downscaled to the regional configuration. The global configuration was set to produce lateral boundary conditions (LBCs) at six-hourly intervals which were then used to drive the regional configuration.

A consistent set of baseline emissions have been used for both configurations by using the same source data and then re-gridding to the global and regional resolutions of the chemistry-climate model. The surface emissions for chemical species were implemented from emission data at 0.5° by 0.5° resolution developed by Lamarque et al. (2010) for the Fifth Coupled Model Inter-comparison Project (CMIP5) report which include reactive gases and aerosols from anthropogenic and biomass burning sources. Both model configurations are driven by decadal mean present-day emissions from Lamarque et al. (2010), representative of the decade centred on 2000. Biogenic emission of isoprene and monoterpenes are calculated interactively

following Pacifico et al. (2011) and the biogenic emissions of methanol and acetone are prescribed, taken from Guenther et al. (1995). A full description of other biogenic emissions and the global and regional configurations can be found in Neal et al. (2017).

The two configurations are consistent in terms of driving meteorology and emissions as discussed above, however a change in model resolution also requires changes to model's dynamical time-step (from 20 min; global resolution to 12 min; regional resolution) as well as some of the parameters in the model parametrisations schemes that are resolution dependent. In this study we assume any such differences to be a model resolution effect. To compare pollutant concentrations simulated at the two resolutions, the global model results were re-gridded to the regional resolution via bi-linear interpolation and differences between the two configurations were then calculated at each grid box. For consistency, all figures, tables and values shown in the following sections show differences calculated as global minus regional.

2.2 Measurement data

Modelled seasonal mean O_3 and $PM_{2.5}$ concentrations for 2007 were evaluated using measurement data from the European Monitoring Evaluation Programme (EMEP) network (ebas.nilu.no). We chose a sub-set of the available EMEP O_3 measurement sites with an altitude less than or equal to 200 m above sea level to focus on near-surface comparisons between measurements and simulated O_3 concentrations (52 sites – Fig. 1). As there are fewer measurements of $PM_{2.5}$ for 2007, all available EMEP measurement sites were used for $PM_{2.5}$ evaluation (25 sites – Fig. 1). All modelled O_3 and $PM_{2.5}$ concentrations shown in this study were taken from the lowest vertical model level which reaches a height of 40 m. To perform an observation-model comparison, simulated pollutant concentrations were extracted at measurement site locations using bi-linear interpolation.

2.3 Health calculations

Annual total mortality estimates associated with long-term exposure to O_3 and $PM_{2.5}$ are frequently calculated by estimating the country-level Attributable Fraction (AF) of mortality, based on concentration-response relationships associated with each pollutant, and then multiplying the AF by the baseline mortality rate. Since we are interested in the effects of changing resolution on pollutant concentration, in our analysis, we focus on the absolute values and differences in the AF between the two resolutions, rather than calculating mortality associated with each pollutant, which also depends on underlying baseline mortality rates. This allows us to isolate the effect of model resolution on health impacts. We note that differences in AF will be the same as the differences in mortality between the two resolutions (expressed as a percentage of total mortality), if calculated as described in this section.

Although there is limited evidence available for the long-term health impacts of O_3 especially in Europe (The UK Committee on the Medical Effects of Air Pollution (COMEAP) 2015), we apply the Health Risks of Air Pollution in Europe – HRAPIE project recommended coefficient for long-term exposure to O_3 (WHO, 2013) to investigate the sensitivity of health

Atmos. Chem. Phys. Discuss., https://doi.org/10.5194/acp-2017-1074
Manuscript under review for journal Atmos. Chem. Phys.
Discussion started: 28 November 2017

Atmospheric Chemistry and Physics Discussions

calculations to model resolutions as used in previous studies (Anenberg et al. 2009; Punger and West 2013; Thompson et al. 2014). The concentration-response coefficient, or β value (Eq.1), for the effects of long-term O_3 exposure on respiratory mortality recommended by HRAPIE is 1.014 (95% Confidence Interval (CI) = 1.005, 1.024) per 10 µg m^{-3} increase in MDA8 O_3 during the warm season (April-September) with a threshold of 70 µg m^{-3} (WHO, 2013). For estimating the health impact of long-term exposure to $PM_{2.5}$ on all-cause (excluding external) mortality, HRAPIE (WHO 2013) recommends a relative risk coefficient of 1.062 (95% CI = 1.040, 1.083) per 10 µg m^{-3} increase in annual average concentrations (with no threshold).

For MDA8 O_3, the risk estimates above, suggested by HRAPIE, are based on data from the American Cancer Society (ACS) cohort (Jerrett et al., 2009) during the warm season re-scaled from 1-hour means to 8-hour means (WHO, 2013). Since MDA8 O_3 concentrations in the summer months exceed 70 µg m^{-3} for most areas included in the ACS study, little information exists on the shape of the concentration-response relationship at low levels. For this reason, following HRAPIE suggestions, only MDA8 O_3 concentrations exceeding 70 µg m^{-3} and averaged between April and September were used in the present study to calculate O_3-related health impacts. For $PM_{2.5}$-related health impacts we use annual averages with no threshold. As the β values used for O_3 and $PM_{2.5}$ are from the ACS cohort, the estimates in this study exclude people younger than 30 years.

For each model resolution, simulated air pollutant concentrations were used to calculate the country-average AF of respiratory or all-cause mortality associated with long-term exposure to O_3 and $PM_{2.5}$, respectively. Specifically, the country-average AF is derived from the country-averaged population-weighted pollutant concentration ($x_{country}$) and concentration-response coefficient (β) as shown in Eq. (1) (e.g. Anenberg et al. 2010; Gowers et al. 2014):

$$AF_{country} = 1 - e^{-\beta x_{country}} \quad (1)$$

The country-averaged population-weighted pollutant concentrations ($x_{country}$) were derived using gridded population data at a resolution of 0.5° (GWPv3), obtained from the Socioeconomic Data and Applications Centre (SEDAC, http://sedac.ciesin.columbia.edu/data/set/gpw-v3-population-count-future-estimates/data-download), following Eq. (2).

$$x_{country} = \frac{\sum_{i \in country} (p_i \times x_i)}{\sum_{i \in country} p_i} \quad (2)$$

Here, x_i represents the pollutant concentration within each model grid-cell i and p_i represents the number of people (aged 30+ years) exposed to the pollutant concentration also at the model grid-cell level. For population-weighted $PM_{2.5}$ concentrations, the simulated $PM_{2.5}$ concentration for each model grid-cell was multiplied by the number of people within the same model grid-cell. This product was then summed for all grid-cells within the country and divided by the total population of the respective country. A similar procedure was used for MDA8 O_3 concentrations. However, for populated–weighted MDA8 O_3 concentrations, 70 µg m^{-3} was first subtracted from the simulated MDA8 O_3 concentration at each grid-cell before multiplying by the population (any resultant negative concentrations were set to zero).

Atmos. Chem. Phys. Discuss., https://doi.org/10.5194/acp-2017-1074
Manuscript under review for journal Atmos. Chem. Phys.
Discussion started: 28 November 2017

3 The impact of model resolution on pollutant concentrations

3.1 The impact of model resolution on seasonal mean O_3: comparison with observations

Modelled and observed means and, standard deviations (SD), normalised mean bias (NMB) and percentage differences between the two resolutions for all four seasons at the 52 EMEP site locations are shown in Table 1. Similarly modelled means, SD and percentage differences between the two resolutions are also shown for all model cells within the European domain (discussed in Section 3.2). Compared to measurements, mean values simulated by the chemistry-climate model across the 52 station locations are lower in winter (DJF) and higher in summer (JJA) and autumn (SON) with NMB values up to -19%, 19% and 27%, respectively. In spring (MAM), simulated mean O_3 concentrations at the regional resolution are closest to observations (NMB = ~ -4 %), whilst in all other three seasons the simulated values at the global resolution are in closer agreement with observations (NMB = ~ -8%, ~24% and ~ 5%, respectively).

For all seasons, the SD of seasonal mean O_3 concentrations, simulated at the two resolutions are more similar to each other than to observations. However, the SD across all 52 sites, simulated at the global resolution is higher than that simulated at the regional resolution.

Modelled versus observed seasonal mean O_3 concentrations for each of the 52 EMEP station locations are shown in Fig. 2, with arrow lengths indicating the change in concentrations when simulated at global versus regional resolutions. For both resolutions, higher O_3 concentrations are simulated during summer compared to observations as noted above (between 50 to 150 µg m^{-3}; Fig. 2). In winter, simulated O_3 concentrations are lower compared to measurements (< 30 µg m^{-3}), and are most similar to observations in spring and autumn in accordance with lower NMB (Table 1).

The magnitude of the differences in simulated O_3 concentrations between the two resolutions varies seasonally, with the smallest (global-regional) differences in summer (green arrows – Fig. 3; -3 % ;Table 1) and the largest difference in spring, as noted above (16 % ;Table 1). Similar differences in July mean O_3 concentrations between a 150 km and a 40 km resolution were also found by Stock et al. (2014). Over the majority of the stations, during winter and spring, O_3 concentrations simulated at the regional resolution are lower than concentrations simulated at the global resolution (downward arrows; Fig. 2, positive difference; Table 1). In contrast during summer and autumn, O_3 concentrations are higher when simulated at the regional resolution (upward arrows; Fig. 2, negative difference; Table 1). These results are analysed further at the seasonal level in Fig. S1 of the Supplement to this article (Supplement S2; Fig. S1).

3.2 The impact of model resolution on seasonal mean O_3: spatial differences

This section extends our investigation to examine the impact of model grid resolution on the spatial distribution of O_3 over the whole of Europe. The seasonal variation in O_3 concentrations simulated at the regional resolution across Europe shows the same features as at the 52 site locations (section 3.1), with highest values in spring and summer (> 50 µg m^{-3} and up to 120 µg m^{-3}; Fig. 3b and 3c, respectively) and lowest values in autumn and winter (<55 µg m^{-3}; Fig. 3a and 3d). In all seasons, except

winter, there is a clear latitudinal gradient with higher O_3 concentrations in southern compared to northern Europe. In winter (Fig. 3a), very low O_3 concentrations are simulated across much of Europe (~30 µg m^{-3}).

For most of Europe, in winter and spring, mean O_3 concentrations are generally higher when simulated at the global compared to the regional resolution (Fig. 3e and 3f, 10% and 6% respectively; Table 1), in agreement with the findings for the sub-set of 52 locations. However parts of northern Scandinavia and the UK, and parts of south-eastern Europe have lower O_3 concentrations simulated at the global resolution in these two seasons. In summer and autumn, O_3 concentrations are slightly lower when simulated at the global compared to the regional resolution (-1% and -4% respectively –Table 1) as found for the sub-set of locations, except in areas of easternmost Europe (especially in autumn) and parts of Spain and Italy (Fig. 3g and 3h). The greatest positive differences in simulated O_3 concentrations, i.e. higher values at the global resolution, are found in winter, especially in the far south of Europe in Spain (~ 20 µg m^{-3}; Fig. 3e). Some of these positive differences are clear around the coastal regions which is likely due to differences in the land/sea mask at the two resolutions, which leads to less deposition over oceanic grid-cells at the global resolution and higher simulated O_3 concentrations compared to the same locations that are designated as land at the regional scale (Coleman et al., 2010). In addition, large positive differences in simulated O_3 concentrations between the two resolutions occur over the Alps, whereby simulated O_3 concentrations are higher at the regional scale (Fig. 3e and 3h). This is most likely due to the differences in orography at the two resolutions with higher elevations at the regional scale leading to higher O_3 concentrations.

Differences in simulated seasonal mean NO_2 concentrations at the two resolutions show similar, but less extensive differences and generally inverse patterns as for O_3 concentrations, with some negative differences, i.e. lower NO_2 values in winter and spring (Fig. 3i and 3j), when simulated at the global compared to the regional resolution. In contrast, in summer and autumn, NO_2 concentrations are higher in some regions when simulated at the global compared to the regional resolution (e.g. Italy; Fig. 3k and 3l). An inverse relationship i.e. a positive difference in O_3 concentrations and a negative difference in NO_2 concentrations is most prominent for locations in Spain (all year around) and Italy (winter and spring) and parts of the Benelux region (southern UK and Netherlands; all year around). This inverse relationship is driven by lower NO_x concentrations at the global resolution which lead to less O_3 titration by NO compared to the regional resolution (Fig. 3i). This in turn results in higher simulated seasonal mean O_3 concentrations at the global resolution compared to the regional resolution (Fig. 3e).

The planetary boundary layer (PBL) height is a key meteorological variable that affects the vertical transport of pollutants from the surface into the free troposphere from where they can then undergo strong horizontal transport. Thus we have also investigated the impact of changing model resolution on PBL height and how this impacts O_3 and NO_2 concentrations. Spatial differences in PBL height between the two resolutions are shown in Section S3, Fig. S2 of the Supplement to this article. In all seasons, over most of western and central Europe and especially in summer, the PBL height is generally lower when simulated at the global resolution (negative differences up to 275m; Fig. S2c). In winter and spring (Fig. S2a and S2b), this lower height corresponds to generally higher O_3 concentrations but also lower NO_2 concentrations simulated at the global resolution, over the same region and vice versa in summer and autumn (Fig. S2c and S2d). If a deeper

PBL is the main driver of pollutant trapping producing higher O_3 levels, then we would also expect NO_2 concentrations to be higher with a lower PBL height at the regional resolution, but their frequent inverse relationship suggest a stronger role for chemistry rather than PBL effects. However, these chemical and physical processes cannot be clearly separated.

In summary, we find a strong seasonal variation in simulated O_3 differences between the two resolutions. Simulated O_3 concentrations at the global resolution are higher in winter and spring and lower in summer and autumn compared to the regional resolution. We also find that in a number of locations, NO_2 concentrations are lower at the global compared to the regional resolution and correspond to higher O_3 concentrations at the global resolution as a result of reduced titration with lower NO_x levels. Orography also plays an important role in some coastal locations, leading to an overestimation of O_3 concentrations. The PBL height differs between the two resolutions especially during summer, with the regional resolution resulting in a deeper boundary layer. However, it is not possible to separate chemistry and mixing effects on simulated O_3 concentrations.

3.3 The impact of model resolution on seasonal mean $PM_{2.5}$ – comparison with observations

Simulated seasonal mean $PM_{2.5}$ concentrations are compared to available EMEP observations at 25 sites (Table 2). Mean values for the observations are fairly similar across all seasons, with values in summer and autumn being slightly lower. $PM_{2.5}$ concentrations simulated at both the global and regional resolutions are lower in winter and higher in summer compared to measurements. In addition, mean $PM_{2.5}$ concentrations simulated at the regional resolution are higher than those simulated at the global resolution except in summer. The global resolution simulates $PM_{2.5}$ levels with the smallest bias during spring (NMB = -0.2%). In contrast, $PM_{2.5}$ concentrations simulated at the regional resolution during spring have a large positive bias (NMB = 31%). Similarly in autumn NMB values are larger for $PM_{2.5}$ concentrations simulated at the regional resolution. We find that the largest bias for both resolutions occurs in summer with the global resolution resulting in a NMB of 70%. Using, a similar regional configuration, Neal et al. (2017) found a year-round small positive bias in simulated $PM_{2.5}$ concentrations averaged over a five year period (2001-2005) at two UK locations. The SD of $PM_{2.5}$ concentrations across the 25 sites is fairly similar between model results and measurements except in winter, when simulated SD values are lower at both resolutions compared to measurements and in autumn, when the SD at the regional resolution is higher compared to measurements.

Modelled versus measured $PM_{2.5}$ concentrations across the 25 individual EMEP stations highlight the low simulated $PM_{2.5}$ concentrations in winter (Section S3, Fig. S3 of the Supplement to this article). Large variations in $PM_{2.5}$ levels between the two resolutions are prominent in spring (-31%; Table 2). Smaller $PM_{2.5}$ concentrations simulated at the global resolution in winter, spring and autumn are apparent (upward arrows; Fig. S3, negative differences; Table 2).

3.4 Impact of model resolution on seasonal mean $PM_{2.5}$: spatial differences

Spatial distributions of $PM_{2.5}$ concentrations, simulated at the regional resolution as well as differences between the two resolutions over the whole European domain are illustrated in Fig. 4. Over the whole domain, $PM_{2.5}$ concentrations simulated at the regional resolution are lowest in winter (Fig. 4a) and highest in spring (Fig. 4b). As for O_3, there is clear latitudinal

gradient with higher $PM_{2.5}$ levels in southern Europe in all seasons. Differences in seasonal mean $PM_{2.5}$ concentrations, between the coarse and fine resolutions, vary seasonally across the European domain with the smallest differences occurring during winter (± 3 μg m^{-3}; Fig. 4e, -8% ; Table 2) in agreement with the findings for the 25 EMEP stations described above (section 3.3). This suggests that at low $PM_{2.5}$ concentrations (~ 8 μg m^{-3}) in winter, model results do not differ greatly when
295 increasing the model resolution from 150 km to 50 km. In spring, $PM_{2.5}$ concentrations simulated at the global are lower than at the regional resolution over large parts of central and western Europe but are slightly higher in easternmost parts of Europe (negative differences ~-10 μg m^{-3} Fig. 4f; -27% Table 2), as found at the 25 EMEP station locations. The opposite result occurs in summer with generally higher $PM_{2.5}$ concentrations simulated at the coarser resolution (positive differences ~ 10 μg m^{-3} Fig. 4g; 29% Table 2). In autumn, the differences in $PM_{2.5}$ concentrations at the two resolutions exhibit a marked east-west
300 contrast, with lower values at the global resolution in western Europe (where the EMEP stations are generally located; Fig. 1) and higher values at the global resolution in eastern Europe (Fig. 4h). While $PM_{2.5}$ concentrations at the 25 EMEP site locations are on average lower when simulated at the global resolution (-23%), over all grid-cells, $PM_{2.5}$ concentrations are higher at the global resolution (8%). This highlights issues with representivity of the EMEP network across Europe, with much fewer EMEP measurement stations for $PM_{2.5}$ in eastern Europe.

305 The seasonality in $PM_{2.5}$ differences, brought about by a change in model horizontal resolution, can be partly explained by differences in PBL height between the two resolutions, as outlined in section 3.2. In particular, the deeper boundary layer in summer simulated at the regional resolution may lead to greater vertical lofting from the surface, producing lower $PM_{2.5}$ levels compared to that simulated at the global resolution. In addition, differences in simulated precipitation (especially smaller-scale convective precipitation) between the two resolutions may be important, through its influence as the
310 dominant mechanism in UKCA for removal of aerosols through wet deposition (O'Connor et al., 2014). Spatial patterns of convective precipitation differences between the two resolutions are shown in Section S3, Fig. S4 of the Supplement to this article. In winter and spring, convective rainfall is higher at the global compared to the regional resolution (Fig. S4a and S4b). Thus removal of $PM_{2.5}$ through wet deposition is greater, producing lower $PM_{2.5}$ concentrations at the coarser resolution (Fig. 4e and 4f). The opposite holds in summer and autumn as the convective rainfall is lower at the global compared to the regional
315 resolution (Fig. S4c and S4d) therefore resulting in higher $PM_{2.5}$ concentrations simulated at the global resolution (Fig. 4g and 4h).

Overall, we also find a large seasonal variation in simulated $PM_{2.5}$ concentrations between the two resolutions, with typically lower levels simulated in winter and spring at the global compared to the regional resolution and the opposite result in summer and autumn. Hence, the seasonality of differences in simulated $PM_{2.5}$ concentrations between the two model
320 resolutions is generally the inverse of that found for O_3 in section 3.3. We find that these seasonal differences can be largely explained by meteorological effects: PBL height differences, especially in summer, and by differences in convective rainfall between the two resolutions.

Atmos. Chem. Phys. Discuss., https://doi.org/10.5194/acp-2017-1074
Manuscript under review for journal Atmos. Chem. Phys.
Discussion started: 28 November 2017

4 Sensitivity of health impact estimates to model resolution

We now examine how the differences in O_3 and $PM_{2.5}$ concentrations simulated at the two resolutions, influence health impact estimations across Europe at the country level. For this analysis we use warm season daily maximum 8-hour running mean (MDA8) O_3 (above 70 µg m^{-3}) and annual-average $PM_{2.5}$ concentrations. To estimate health impacts, air pollution concentrations (with an averaging period consistent with that used in epidemiological studies) are combined with population estimates and concentration-response coefficients (Section 2.3).

4.1 Warm season MDA8 O_3 and annual-average $PM_{2.5}$ concentrations

Statistics for warm season MDA8 O_3 and annual $PM_{2.5}$ concentrations compared between EMEP measurements and model results at the two resolutions are provided in Section S1, Table S1 of the Supplement to this article. Mean simulated MDA8 O_3 levels in the warm season at the 52 EMEP locations for both resolutions, are higher compared to observations (NMB = 11% and 9 %; Table S1), in agreement with our findings for summer and autumn mean O_3 levels (c.f., Table S1, Table 1). The SD is also higher for both resolutions compared to observations. However, in contrast with summer mean O_3 levels, mean simulated MDA8 O_3 concentrations are 1 % higher at the global compared to the regional resolution at the 52 EMEP site locations (Table S1). Simulated annual mean $PM_{2.5}$ concentrations are also higher compared to observations at the 25 locations (NMB =~10-20%; Table S1) with concentrations being 9% lower at the global compared to the regional resolution. This represents the net effect of seasonality in NMB shown in Table 2.

Differences in warm season MDA8 O_3 and annual mean $PM_{2.5}$ concentrations, simulated at the global and regional resolution, are shown in Fig. 5. The spatial distribution of differences in warm season MDA8 O_3 between the two resolutions (Fig. 5a) is most similar to the distribution of differences in summer mean O_3 concentrations (Fig. 3g). Differences in MDA8 O_3 concentrations range from ~ -7 µg m^{-3} in Northeast Europe to ~ +20 µg m^{-3} in Southern Europe, UK and Ireland (Fig. 5a). We note that if a different time-averaging period was chosen e.g., annual as opposed to warm season, the spatial patterns of MDA8 O_3 differences would alter considerably due to the seasonal variation displayed in Figure 3.

The spatial distribution of differences in annual mean $PM_{2.5}$ concentrations between the two resolutions (Fig. 5b) are most similar to the spatial distribution of differences in spring and especially autumn mean $PM_{2.5}$ concentrations notably with an east-west gradient (Fig. 5). Differences in $PM_{2.5}$ concentrations between the two resolutions range from ~ -8 µg m^{-3} in the southwestern part of Europe and Cyprus to ~ +4 µg m^{-3} in north and eastern Europe (Fig. 5b).

4.2 Effect of applying population-weighting to MDA8 O_3 and annual $PM_{2.5}$ concentrations

The warm season MDA8 O_3 concentrations and annual mean $PM_{2.5}$ concentrations, simulated at both resolutions, were weighted by population totals for each country to produce country average population-weighted concentrations (Section 2.3). Figure 6a shows the impact of the two resolutions on country-average warm season average MDA8 O_3 and the corresponding

population-weighted MDA8 O_3 concentrations. Similarly differences in annual mean $PM_{2.5}$ concentrations between the two resolutions for non-population-weighted and population-weighted concentrations are shown in Fig. 6b.

Population-weighting of pollutant concentrations has different impacts across the European countries (Fig. 6a and 6b). In many countries, differences in population-weighted pollutant concentrations between the two resolutions are enhanced (i.e. larger positive or more negative differences) relative to non-population-weighted pollutant concentrations. However, in some countries population-weighting may reduce the positive or negative difference between the two resolutions. We examine several cases below.

For warm season MDA8 O_3 concentrations, the largest negative differences, implying lower MDA8 O_3 levels using global compared to the regional resolution results, occur in eastern Europe (Fig. 5a). Hence, the largest negative differences in non-population-weighted and population-weighted MDA8 O_3 concentrations are found in eastern European countries (Fig. 6a). The difference between the two resolutions is greatest when population-weighting is applied. This is generally due to slightly lower population-weighted MDA8 O_3 concentrations compared to MDA8 O_3 concentrations derived from the global resolution results (Section S3, Fig. S5a of the Supplement to this article).

In the Netherlands warm season non-population-weighted MDA8 O_3 is also lower when derived from global compared to regional resolution results (negative difference; Fig. 5a, 6a). However population-weighted MDA8 O_3 concentrations are higher when derived from the global resolution results (Fig. 6a). This is caused by lower MDA8 O_3 concentrations simulated at the regional resolution when applying population-weighting (Fig. S5a). This suggests that in populated regions, MDA8 O_3 concentrations simulated at the regional resolution are lower which might be linked to higher NO_2 concentrations.

Warm season MDA8 O_3 show the largest positive differences, with higher values simulated at the global resolution, for southern Europe and the UK/Ireland (Fig 5a). Thus, the largest positive differences for non-population-weighted and population-weighted MDA8 O_3 concentrations occurs in south European countries (Fig. 6a). Population–weighed MDA8 O_3 concentrations in Portugal are higher compared to MDA8 O_3 concentrations at the global but lower at the regional resolution (Fig. S5a). This suggests that, at the global resolution, areas with high levels of O_3 are co-located with high population densities whilst at the regional resolution areas with lower levels of O_3 are co-located with high population densities.

Annual-average $PM_{2.5}$ concentrations show the largest negative differences, with higher values simulated at the regional resolution, in parts of western Europe (Fig. 5b). Hence, the largest negative non-population-weighted and population-weighted annual mean $PM_{2.5}$ concentrations are found for Cyprus, Italy and Spain (Fig. 6b). Conversely, higher annual-average $PM_{2.5}$ levels are simulated at the global resolution in eastern and northern Europe (Fig. 5b), hence larger positive non-population-weighted and population-weighted annual mean $PM_{2.5}$ concentrations occur for countries in eastern Europe and northern Europe (Fig. 6b).

In Cyprus, population-weighted annual mean $PM_{2.5}$ concentrations simulated at the regional resolution are higher compared to concentrations with no population-weighting, due to denser populations being co-located with areas of higher $PM_{2.5}$ levels (Fig. S5b). In Croatia, population-weighted annual mean $PM_{2.5}$ concentrations simulated at the global resolution

are greater than $PM_{2.5}$ concentrations with no population-weighted, again due to denser populations in regions of high concentrations but in this case when simulated at the global resolution (Fig. S5b). In a few countries (e.g. Switzerland), differences in population-weighted annual mean $PM_{2.5}$ concentrations between the two resolutions have an opposite sign to differences between concentration with no population-weighting (Fig. 6b). This indicates that annual mean $PM_{2.5}$ concentrations simulated at the regional resolution are high in densely populated regions but are low in these same regions at the global resolution.

4.3 Attributable fraction of mortality associated with long-term exposure to O_3

The Attributable Fraction (AF) associated with long-term exposure to MDA8 O_3, expressed as a percentage of total respiratory mortality and simulated at both resolutions, was calculated for each country (Fig. 7a), using the population-weighted warm season MDA8 O_3 concentrations (Fig. 6a) as discussed in Section 2.3. For both resolutions, the estimated AF is shown for each country, with the 95% confidence interval (95% C.I.) representing uncertainties associated only with the concentration-response coefficient (β) used (shown in grey). For all the countries considered, irrespective of the model resolution used, the AF of total respiratory mortality ranges from 1% (95% C.I. 0% - 2%) in Finland to 11 % (95% C.I. 4% - 18%) in Cyprus (Fig. 7a). Differences in AF between the countries are solely attributed to differences in population-weighted MDA8 O_3 concentrations. Thus, countries with the highest population-weighted concentrations also have the highest AF. Similarly countries with the highest differences in population-weighted MDA8 O_3 concentrations between the two resolutions also have the largest differences in AF between the global and regional resolution.

The differences in AF associated with long-term exposure to warm season MDA8 O_3, simulated at the two resolutions, are shown in Fig. 7b. These values highlight the sensitivity of respiratory mortality attributable to long-term exposure to O_3 to a change in model resolution.

For most of northern and eastern Europe, the AF at the global resolution is lower than that at the regional resolution (negative differences; Fig. 7b) as for differences in population-weighted warm season MDA8 O_3 concentrations in the same countries (Fig. 6a). In contrast, the AF at the global resolution is higher than that at the regional resolution for countries in southern Europe (positive differences, Fig. 7b). Differences in AF range from -0.9% (95% C.I. -0.3% to -1.5%) in Poland to +2.6% (95% C.I. 1.0% to 4.1%) in Portugal (Fig. 7b) which directly correspond to the countries having the lowest and highest difference in population-weighted MDA8 O_3 concentration respectively (Fig. 6a; Note, although the differences in AF between the two resolution appear to be low, these are percentages of total mortality). For approximately half of the European countries, the AF is higher for the global resolution compared to the regional resolution and vice versa. The uncertainty associated with the concentration-response coefficient used does not alter the sign of the difference of AF between the two model resolutions.

Atmos. Chem. Phys. Discuss., https://doi.org/10.5194/acp-2017-1074
Manuscript under review for journal Atmos. Chem. Phys.
Discussion started: 28 November 2017

4.4 Attributable Fraction associated with long-term exposure to $PM_{2.5}$

The fraction of all-cause (excluding external) mortality attributable to long-term exposure to $PM_{2.5}$, is shown as percentages for each country in Fig. 8a. The AF for all countries, irrespective of the resolution used, ranges from 2% (95% C.I. 1% - 3%) in Iceland to 15% (95% C.I. 10% - 19%) in Cyprus (Fig. 8a). Differences in AF between the two resolutions are shown in Fig. 8b. Since the variability in AF differences across the countries is caused by variability in population-weighted annual mean PM2.5 differences, Cyprus and countries in parts of western Europe have the largest negative difference in percentage AF (Fig. 8b). In contrast, countries in eastern and northern Europe have the largest positive difference in percentage AF (Fig. 8b). These differences range from -4.7% (95% C.I. -6.1% to -3.2%) in Cyprus to 2.8% (95% C.I. 1.9% to 3.7%) in Croatia. Over most countries, annual mean population-weighted $PM_{2.5}$ concentrations are higher (positive difference; Fig. 6b) for the global compared to the regional resolution, thus resulting in a higher AF when using the global resolution results.

Our results are consistent with other studies, but not all, that examine the impact of model resolution on health estimates associated with long-term exposure to $PM_{2.5}$. Using concentrations simulated at the 36 km resolution, Punger and West (2013) find that the U.S. national health estimate is higher (11%) than the estimate at 12 km resolution. Li et al. (2016) also show that averaged over the US, a coarse grid resolution (~ 200 km) results in a health estimate that is lower (8%) than the estimated based on the fine scale model results (~ 50 km), in contrast to our findings averaged across Europe. All these studies are conducted in the U.S. and hence definitive comparisons cannot be made with our results for Europe. Note, similar to O_3, the uncertainty associated with the concentration-response coefficient for $PM_{2.5}$ does not alter the sign of the difference of AF between the two model resolutions (Fig. 8b).

In summary, our results suggest that differences in AF health estimates between global and regional resolutions vary across the different European countries with clear differences between southern and eastern Europe for exposure to warm season MDA8 O_3 and west-east differences for exposure to annual-average $PM_{2.5}$ due to the dependence of AF on populated weighted MDA8 O_3 and annual $PM_{2.5}$ concentrations.

5 Conclusions

Chemistry-climate model simulations were performed at two resolutions: a global resolution (~ 140 km) and a regional resolution (~ 50 km) over Europe to quantify the impact of horizontal model resolution on simulated O_3 and $PM_{2.5}$ concentrations by season; and on the associated Attributable Fraction (AF) of mortality due to long-term exposure to these two pollutants. Simulated O_3 concentrations are lower in winter and higher in summer and autumn compared to measurements at both model resolutions. Results show a strong seasonal influence in the mean O_3 differences between the two resolutions. Simulated O_3 concentrations averaged across Europe at the global resolution are higher in winter and spring (10% and 6%, respectively), and lower in summer and autumn (-1% and -4%, respectively) compared to the regional resolution. In contrast during winter and spring, NO_2 concentrations are lower in some areas at the global compared to the regional configuration, whilst in summer and autumn, there are more locations where NO_2 concentrations are higher at the global resolution. The

lower O_3 concentrations simulated at the regional compared to the global resolution can be partly explained by these higher NO_2 levels that enhance titration of O_3 at this finer resolution. The PBL height also differs between the two resolutions and may also account for differences in O_3 concentrations; however, it is not possible to clearly separate the effects of chemistry and mixing on simulated O_3.

Differences in $PM_{2.5}$ concentrations simulated at the two resolutions also vary seasonally. Modelled $PM_{2.5}$ concentrations are lower in winter and higher in summer compared to measurements at both resolutions. Simulated seasonal mean $PM_{2.5}$ concentrations averaged across Europe during winter and spring are lower at the global compared to the regional resolution (-8% and -27%, respectively) but higher in summer and autumn (29% and 8%, respectively). This seasonality in Europe-average differences in $PM_{2.5}$ concentrations is opposite to that found for differences in O_3 concentrations between the two resolutions. Differences in $PM_{2.5}$ concentrations simulated at the two resolutions are also influenced by PBL height, especially in summer when a deeper boundary layer at the regional resolution leads to greater lofting and lower $PM_{2.5}$ concentrations. Furthermore, in all seasons, the differences in $PM_{2.5}$ levels between the two resolutions are closely related to differences in the convective rainfall rate. In winter and spring, the convective rainfall at the global resolution is higher than that at the regional resolution thus resulting in lower $PM_{2.5}$ concentrations. The opposite result holds in summer and autumn.

Results show that differences in warm season mean MDA8 O_3 concentrations between the two resolutions are similar to summer mean differences in simulated O_3 concentrations, with spatial patterns of differences reveal clear and important contrasts. Warm season MDA8 O_3 levels are higher in most of southern Europe as well as the UK and Ireland, but lower in other areas of northern as well as eastern Europe when simulated at the global resolution compared to the regional resolution. On the other hand, annual average $PM_{2.5}$ concentrations are higher across most of northern and eastern Europe but lower over parts of southwest Europe at the global compared to the regional resolution.

Weighting the pollutant concentrations at both resolutions with the population within each country, results in some added differences between concentrations at the two resolutions which also vary across the countries. In many countries, weighting by population enhances either positive or negative differences in warm season MDA8 O_3 or annual mean $PM_{2.5}$ concentrations between the two resolution, which suggests that high levels of pollutant concentrations coincide with high population density at one resolution but low pollutant concentrations are co-located with high population density at the other resolution. Population-weighting pollutant concentrations also reduces differences between global and regional resolution results in some countries.

The AF of respiratory mortality associated with long-term exposure to warm season MDA8 O_3 and annual mean $PM_{2.5}$ is also sensitive to resolution as is it is solely driven by the simulated population-weighted pollutant concentrations. For the AF associated with long-term exposure to O_3, countries in northern as well as eastern Europe have lower AF values at the global compared to the regional resolution whilst the opposite result occurs for other countries in southern Europe and Ireland. For the AF associated with long-term exposure to $PM_{2.5}$, a few countries in southwestern Europe and Cyprus have lower AF values for $PM_{2.5}$ concentrations simulated at the global resolution whilst more countries especially in eastern and northern Europe show a higher AF when using $PM_{2.5}$ concentrations simulated at the global resolution.

Overall, differences in the country-average AF associated with long term exposure to MDA8 O_3 range between -0.9 % and +2.6 % while differences in the AF associated with long-term exposure to annual mean $PM_{2.5}$ range from -4.7% to +2.8 % of the total baseline mortality. This result emphasizes the importance of model horizontal resolution when conducting country specific health impact studies. We also note that the impacts of a 95% C.I. in concentration-response coefficient is smaller than the impact of the model horizontal resolution.

Our calculation for O_3 health impacts only considers warm-season MDA8 O_3 impacts however these may differ to annual MDA8 O_3 impacts because of seasonal differences in simulated O_3 with resolution highlighted in this study. In addition, for our study we apply the same concentration-response coefficient to all populations and assumed that for $PM_{2.5}$-related health impacts, all $PM_{2.5}$ components have the same impact on mortality. Future research focusing on the sensitivity of AF changes to different averaging periods or seasons would be beneficial. In addition, the use of concentration-response coefficients that are derived from European cohort data would be useful, although such data are limited. Nonetheless this study provides one of the first insights as to how air pollution related health impacts over Europe are influenced by the model resolution used to simulate pollutant concentrations.

Acknowledgements

Sara Fenech's PhD was funded by Public Health England. The development of the United Kingdom Chemistry and Aerosol (UKCA) model and Fiona M. O'Connor are supported by the Joint UK BEIS/Defra Met Office Hadley Centre Climate Programme (GA01101).

References

Anenberg, S. C., West, J. J., Fiore, A. M., Jaffe, D. A., Prather, M., Bergmann, D., Cuvelier, K. and Dentener, F. J.: Intercontinental Impacts of Ozone Pollution on Human Mortality, Environ. Sci. Technol., 43(17), 6482–6487, doi:10.1029/2008GM000741/summary, 2009.

Anenberg, S. C., Horowitz, L. W., Tong, D. Q. and West, J. J.: An estimate of the global burden of anthropogenic ozone and fine particulate matter on premature human mortality using atmospheric modeling, Environ. Health Perspect., 118(9), 1189–1195, doi:10.1289/ehp.0901220, 2010.

Arunachalam, S., Wang, B., Davis, N., Baek, B. H. and Levy, J. I.: Effect of chemistry-transport model scale and resolution on population exposure to PM2.5 from aircraft emissions during landing and takeoff, Atmos. Environ., 45(19), 3294–3300, doi:10.1016/j.atmosenv.2011.03.029, 2011.

Bellouin, N., Rae, J., Jones, A., Johnson, C., Haywood, J. and Boucher, O.: Aerosol forcing in the Climate Model Intercomparison Project (CMIP5) simulations by HadGEM2-ES and the role of ammonium nitrate, J. Geophys. Res. Atmos., 116(20), 1–25, doi:10.1029/2011JD016074, 2011.

Brook, R. D., Rajagopalan, S., Pope, C. A., Brook, J. R., Bhatnagar, A., Diez-Roux, A. V., Holguin, F., Hong, Y., Luepker, R. V., Mittleman, M. a., Peters, A., Siscovick, D., Smith, S. C., Whitsel, L. and Kaufman, J. D.: Particulate matter air pollution and cardiovascular disease: An update to the scientific statement from the american heart association, Circulation, 121(21), 2331–2378, doi:10.1161/CIR.0b013e3181dbece1, 2010.

Brown, A., Milton, S., Cullen, M., Golding, B., Mitchell, J. and Shelly, A.: Unified modeling and prediction of weather and climate: A 25-year journey, Bull. Am. Meteorol. Soc., 93(12), 1865–1877, doi:10.1175/BAMS-D-12-00018.1, 2012.

Cohen, A. J., Anderson, H. R., Ostro, B., Pandey, K. D., Krzyzanowski, M., Künzli, N., Gutschmidt, K., Iii, C. A. P., Romieu, I., Samet, J. M. and Smith, K. R.: Urban Air Pollution, in Urban air pollution. In: Comparative quantification of health risks: global and regional burden of disease due to selected major risk factors., edited by M. Ezzati, A. Lopez, A. Rodgers, and C. Murray, pp. 1353–1434, World Health Organization, Geneva., 2004.

Coleman, L., Varghese, S., Tripathi, O. P., Jennings, S. G. and O'Dowd, C. D.: Regional-Scale Ozone Deposition to North-East Atlantic Waters, Adv. Meteorol., 2010, 1–16, doi:10.1155/2010/243701, 2010.

Colette, A., Bessagnet, B., Vautard, R., Szopa, S., Rao, S., Schucht, S., Klimont, Z., Menut, L., Clain, G., Meleux, F., Curci, G. and Rouïl, L.: European atmosphere in 2050, a regional air quality and climate perspective under CMIP5 scenarios, Atmos. Chem. Phys., 13(15), 7451–7471, doi:10.5194/acp-13-7451-2013, 2013.

Collins, W. J., Bellouin, N., Doutriaux-Boucher, M., Gedney, N., Halloran, P., Hinton, T., Hughes, J., Jones, C. D., Joshi, M., Liddicoat, S., Martin, G., O'Connor, F., Rae, J., Senior, C., Sitch, S., Totterdell, I., Wiltshire, A. and Woodward, S.: Development and evaluation of an Earth-system model – HadGEM2, Geosci. Model Dev. Discuss., 4(2), 997–1062, doi:10.5194/gmdd-4-997-2011, 2011.

COMEAP: Quantification of Mortality and Hospital Admissions Associated with Ground- level Ozone., 2015.

Fang, Y., Naik, V., Horowitz, L. W. and Mauzerall, D. L.: Air pollution and associated human mortality: The role of air pollutant emissions, climate change and methane concentration increases from the preindustrial period to present, Atmos. Chem. Phys., 13(3), 1377–1394, doi:10.5194/acp-13-1377-2013, 2013.

Folberth, G. A., Abraham, N. L., Johnson, C. E., Morgenstern, O., O'Connor, F. M., Pacifico, F., Young, P. A., Collins, W. J. and Pyle, J. a.: Evaluation of the new UKCA climate-composition model. Part III. Extension to Tropospheric Chemistry and Biogeochemical Coupling between Atmosphere and Biosphere, In prep.

Forouzanfar, M. H., Afshin, A., Alexander, L. T., Biryukov, S., Brauer, M., Cercy, K., Charlson, F. J., Cohen, A. J., Dandona, L., Estep, K., Ferrari, A. J., Frostad, J. J., Fullman, N., Godwin, W. W., Griswold, M., Hay, S. I., Kyu, H. H., Larson, H. J., Lim, S. S., Liu, P. Y., Lopez, A. D., Lozano, R., Marczak, L., Mokdad, A. H., Moradi-Lakeh, M., Naghavi, M., Reitsma, M. B., Roth, G. A., Sur, P. J., Vos, T., Wagner, J. A., Wang, H., Zhao, Y., Zhou, M., Barber, R. M., Bell, B., Blore, J. D., Casey, D. C., Coates, M. M., Cooperrider, K., Cornaby, L., Dicker, D., Erskine, H. E., Fleming, T., Foreman, K., Gakidou, E., Haagsma, J. A., Johnson, C. O., Kemmer, L., Ku, T., Leung, J., Masiye, F., Millear, A., Mirarefin, M., Misganaw, A., Mullany, E., Mumford, J. E., Ng, M., Olsen, H., Rao, P., Reinig, N., Roman, Y., Sandar, L., Santomauro, D. F., Slepak, E. L., Sorensen, R. J. D., Thomas, B. A., Vollset, S. E., Whiteford, H. A., Zipkin, B., Murray, C. J. L., Mock, C. N., Anderson,

B. O., Futran, N. D., Anderson, H. R., Bhutta, Z. A., Nisar, M. I., Akseer, N., Krueger, H., Gotay, C. C., Kissoon, N., Kopec, J. A., Pourmalek, F., Burnett, R., Abajobir, A. A., Knibbs, L. D., Veerman, J. L., Lalloo, R., Scott, J. G., Alam, N. K. M., Gouda, H. N., Guo, Y., McGrath, J. J., Charlson, F. J., Erskine, H. E., Jeemon, P., Dandona, R., Goenka, S., Kumar, G. A., et al.: Global, regional, and national comparative risk assessment of 79 behavioural, environmental and occupational, and metabolic risks or clusters of risks, 1990–2015: a systematic analysis for the Global Burden of Disease Study 2015, Lancet, 388(10053), 1659–1724, doi:10.1016/S0140-6736(16)31679-8, 2016.

Gowers, A M., Miller, B. G. and Stedman, J. R.: Estimating Local Mortality Burdens associated with Particulate Air Pollution. [online] Available from: http://www.hpa.org.uk/webc/HPAwebFile/HPAweb_C/1317141074607, 2014.

Guenther, A., Hewitt, C. N., Erickson, D., Fall, R., Geron, C., Graedel, T., Harley, P., Klinger, L., Lerdau, M., McKay, W. A., Pierce, T., Scholes, B., Steinbrecher, R., Tallamraju, R., Taylor, J. and Zimmerman, P.: A global model of natural volatile organic compound emissions, J. Geophys. Res., 100(D5), 8873, doi:10.1029/94JD02950, 1995.

Jerrett, M., Burnett, R. T., Pope, C. A., Ito, K., Thurston, G., Krewski, D., Shi, Y., Calle, E. and Thun, M.: Long-Term Ozone Exposure and Mortality, N. Engl. J. Med., 360(11), 1085–1095, doi:10.1056/NEJMoa0803894, 2009.

Jones, A., Roberts, D. L., Woodage, M. J. and Johnson, C. E.: Indirect sulphate aerosol forcing in a climate model with an interactive sulphur cycle, J. Geophys. Res., 106, 20293–20310, 2001.

Krewski, D.: Extended Follow-Up and Spatial Analysis of the American Cancer Society Study Linking Particulate Air Pollution and Mortality., 2009.

Lamarque, J. F., Bond, T. C., Eyring, V., Granier, C., Heil, a., Klimont, Z., Lee, D., Liousse, C., Mieville, a., Owen, B., Schultz, M. G., Shindell, D., Smith, S. J., Stehfest, E., Van Aardenne, J., Cooper, O. R., Kainuma, M., Mahowald, N., McConnell, J. R., Naik, V., Riahi, K. and Van Vuuren, D. P.: Historical (1850-2000) gridded anthropogenic and biomass burning emissions of reactive gases and aerosols: Methodology and application, Atmos. Chem. Phys., 10(15), 7017–7039, doi:10.5194/acp-10-7017-2010, 2010.

Lelieveld, J., Evans, J. S., Fnais, M., Giannadaki, D. and Pozzer, A.: The contribution of outdoor air pollution sources to premature mortality on a global scale., Nature, 525, 367–71, doi:10.1038/nature15371, 2015.

Li, Y., Henze, D. K., Jack, D. and Kinney, P. L.: The influence of air quality model resolution on health impact assessment for fine particulate matter and its components, Air Qual. Atmos. Heal., 9(1), 51–68, doi:10.1007/s11869-015-0321-z, 2016.

Lock, A. P., Brown, A. R., Bush, M. R., Martin, G. M. and Smith, R. N. B.: A New Boundary Layer Mixing Scheme. Part I: Scheme Description and Single-Column Model Tests, Mon. Weather Rev., 128(9), 3187–3199, doi:10.1175/1520-0493(2000)128<3187:ANBLMS>2.0.CO;2, 2000.

Markakis, K., Valari, M., Perrussel, O., Sanchez, O. and Honore, C.: Climate-forced air-quality modeling at the urban scale: sensitivity to model resolution, emissions and meteorology, Atmos. Chem. Phys., 15(13), 7703–7723, doi:10.5194/acp-15-7703-2015, 2015.

Morgenstern, O., Braesicke, P., O'Connor, F. M., Bushell, A. C., Johnson, C. E., Osprey, S. M. and Pyle, J. A.: Evaluation of the new UKCA climate-composition model – Part 1: The stratosphere, Geosci. Model Dev., 2(1), 43–57, doi:10.5194/gmd-

580 2-43-2009, 2009.

Moufouma-Okia, W. and Jones, R.: Resolution dependence in simulating the African hydroclimate with the HadGEM3-RA regional climate model, Clim. Dyn., 44(3–4), 609–632, doi:10.1007/s00382-014-2322-2, 2014.

Neal, L. S., Dalvi, M., Folberth, G., McInnes, R. N., Agnew, P., O'Connor, F. M., Savage, N. H. and Tilbee, M.: A description and evaluation of an air quality model nested within global and regional composition-climate models using MetUM, Geosci.
585 Model Dev., 10, 3941–3962, doi:10.5194/gmd-2017-73, 2017.

O'Connor, F. M., Johnson, C. E., Morgenstern, O., Abraham, N. L., Braesicke, P., Dalvi, M., Folberth, G. a., Sanderson, M. G., Telford, P. J., Voulgarakis, a., Young, P. J., Zeng, G., Collins, W. J. and Pyle, J. a.: Evaluation of the new UKCA climate-composition model-Part 2: The troposphere, Geosci. Model Dev., 7, 41–91, doi:10.5194/gmd-7-41-2014, 2014.

Pacifico, F., Harrison, S. P., Jones, C. D., Arneth, A., Sitch, S., Weedon, G. P., Barkley, M. P., Palmer, P. I., Serça, D.,
590 Potosnak, M., Fu, T. M., Goldstein, A., Bai, J. and Schurgers, G.: Evaluation of a photosynthesis-based biogenic isoprene emission scheme in JULES and simulation of isoprene emissions under present-day climate conditions, Atmos. Chem. Phys., 11(9), 4371–4389, doi:10.5194/acp-11-4371-2011, 2011.

Punger, E. M. and West, J. J.: The effect of grid resolution on estimates of the burden of ozone and fine particulate matter on premature mortality in the United States., Air Qual. Atmos. Health, 6(3), 563–573, doi:10.1007/s11869-013-0197-8, 2013.

595 Schaap, M., Cuvelier, C., Hendriks, C., Bessagnet, B., Baldasano, J. M., Colette, a., Thunis, P., Karam, D., Fagerli, H., Graff, a., Kranenburg, R., Nyiri, a., Pay, M. T., Rouïl, L., Schulz, M., Simpson, D., Stern, R., Terrenoire, E. and Wind, P.: Performance of European chemistry transport models as function of horizontal resolution, Atmos. Environ., 112, 90–105, doi:10.1016/j.atmosenv.2015.04.003, 2015.

Silva, R. A, West, J. J., Zhang, Y., Anenberg, S. C., Lamarque, J.-F., Shindell, D. T., Collins, W. J., Dalsoren, S., Faluvegi,
600 G., Folberth, G., Horowitz, L. W., Nagashima, T., Naik, V., Rumbold, S., Skeie, R., Sudo, K., Takemura, T., Bergmann, D., Cameron-Smith, P., Cionni, I., Doherty, R. M., Eyring, V., Josse, B., MacKenzie, I. a, Plummer, D., Righi, M., Stevenson, D. S., Strode, S., Szopa, S. and Zeng, G.: Global premature mortality due to anthropogenic outdoor air pollution and the contribution of past climate change, Environ. Res. Lett., 8, 1748–9326, doi:10.1088/1748-9326/8/3/034005, 2013.

Stock, Z. S., Russo, M. R. and Pyle, J. A.: Representing ozone extremes in European megacities: the importance of resolution
605 in a global chemistry climate model, Atmos. Chem. Phys., 14, 3899–3912, doi:10.5194/acp-14-3899-2014, 2014.

Thompson, T. M., Saari, R. K. and Selin, N. E.: Air quality resolution for health impact assessment: influence of regional characteristics, Atmos. Chem. Phys., 14, 969–978, doi:10.5194/acp-14-969-2014, 2014.

Tie, X., Brasseur, G. and Ying, Z.: Impact of model resolution on chemical ozone formation in Mexico City: application of the WRF-Chem model, Atmos. Chem. Phys., 10(18), 8983–8995, doi:10.5194/acp-10-8983-2010, 2010.

610 Turner, M. C., Jerrett, M., Pope, C. A., Krewski, D., Gapstur, S. M., Diver, W. R., Beckerman, B. S., Marshall, J. D., Su, J., Crouse, D. L. and Burnett, R. T.: Long-Term Ozone Exposure and Mortality in a Large Prospective Study, Am. J. Respir. Crit. Care Med., 193(10), 1134–1142, doi:10.1164/rccm.201508-1633OC, 2016.

Valari, M. and Menut, L.: Does an Increase in Air Quality Models' Resolution Bring Surface Ozone Concentrations Closer to

Reality?, J. Atmos. Ocean. Technol., 25(11), 1955–1968, doi:10.1175/2008JTECHA1123.1, 2008.

Walters, D. N., Best, M. J., Bushell, A. C., Copsey, D., Edwards, J. M., Falloon, P. D., Harris, C. M., Lock, A. P., Manners, J. C., Morcrette, C. J., Roberts, M. J., Stratton, R. A., Webster, S., Wilkinson, J. M., Willett, M. R., Boutle, I. A., Earnshaw, P. D., Hill, P. G., MacLachlan, C., Martin, G. M., Moufouma-Okia, W., Palmer, M. D., Petch, J. C., Rooney, G. G., Scaife, A. A. and Williams, K. D.: The Met Office Unified Model Global Atmosphere 3.0/3.1 and JULES Global Land 3.0/3.1 configurations, Geosci. Model Dev., 4(4), 919–941, doi:10.5194/gmd-4-919-2011, 2011.

West, J. J., Naik, V., Horowitz, L. W. and Fiore, a. M.: Effect of regional precursor emission controls on long-range ozone transport – Part 2: steady-state changes in ozone air quality and impacts on human mortality, Atmos. Chem. Phys. Discuss., 9, 6095–6107, doi:10.5194/acpd-9-7079-2009, 2009.

WHO: Health Risks of Air Pollution in Europe – HRAPIE project: Recommendations for concentration-response functions for cost-benefit analysis of particulate matter, ozone and nitrogen dioxide. [online] Available from: http://www.euro.who.int/__data/assets/pdf_file/0006/238956/Health-risks-of-air-pollution-in-Europe-HRAPIE-project,-Recommendations-for-concentrationresponse-functions-for-costbenefit-analysis-of-particulate-matter,-ozone-and-nitrogen-dioxide., 2013.

Yu, K., Jacob, D. J., Fisher, J. a., Kim, P. S., Marais, E. a., Miller, C. C., Travis, K. R., Zhu, L., Yantosca, R. M., Sulprizio, M. P., Cohen, R. C., Dibb, J. E., Fried, A., Mikoviny, T., Ryerson, T. B., Wennberg, P. O. and Wisthaler, A.: Sensitivity to grid resolution in the ability of a chemical transport model to simulate observed oxidant chemistry under high-isoprene conditions, Atmos. Chem. Phys., 16(7), 4369–4378, doi:10.5194/acp-16-4369-2016, 2016.

Atmos. Chem. Phys. Discuss., https://doi.org/10.5194/acp-2017-1074
Manuscript under review for journal Atmos. Chem. Phys.
Discussion started: 28 November 2017

Atmospheric Chemistry and Physics Discussions

635

Table 1: Statistical results comparing seasonal mean O_3 concentrations simulated at the global and regional resolutions to observations from 52 stations within the EMEP network in 2007. Statistical results for all model grid-cells of both resolutions are also shown. Percentage differences between the two model resolutions are calculated as ($O_{3\ \text{global resolution}} - O_{3\ \text{regional resolution}}$)/($O_{3\ \text{global resolution}}$).

			52 sites		all grid-cells	
Season		**Obs.**	**Model**		**Model**	
			140 km	**50 km**	**140 km**	**50 km**
DJF	Mean (µg m^{-3})	52.8	48.5	42.6	35.1	31.7
	NMB (%)		-8.1	-19.2		
	SD (µg m^{-3})	11.0	17.0	16.0	17.3	16.5
	Difference (%)		12		10	
MAM	Mean (µg m^{-3})	70.4	80.7	67.9	75.7	71.5
	NMB (%)		14.6	-3.6		
	SD (µg m^{-3})	8.9	13.7	12.8	12.9	12.9
	Difference (%)		16		6	
JJA	Mean (µg m^{-3})	63.6	78.6	80.8	84.4	85.6
	NMB (%)		23.7	27.1		
	SD (µg m^{-3})	10.2	16.3	15.1	20.6	20.5
	Difference (%)		-3		-1	
SON	Mean (µg m^{-3})	46.3	48.6	55.0	52.7	54.9
	NMB (%)		4.9	18.8		
	SD (µg m^{-3})	10.2	15.0	14.2	15.2	14.1
	Difference (%)		-13		-4	

640

Atmos. Chem. Phys. Discuss., https://doi.org/10.5194/acp-2017-1074
Manuscript under review for journal Atmos. Chem. Phys.
Discussion started: 28 November 2017

Atmospheric Chemistry and Physics Discussions

Table 2: Statistical results comparing seasonal mean $PM_{2.5}$ concentrations simulated at the global and regional resolutions to observations from 25 stations within the EMEP network in 2007. Statistical results for all model grid-cells of both resolutions are also shown. Percentage differences between the two model resolutions are calculated as ($PM_{2.5\ global\ resolution} - PM_{2.5\ regional\ resolution}$)/($PM_{2.5\ global\ resolution}$).

Season		25 sites			All grid-cells	
		Obs.	Model		Model	
			140 km	50 km	140 km	50 km
DJF	Mean (μg m^{-3})	12.1	8.3	9.5	5.1	5.5
	NMB (%)		-31.0	-21.3		
	SD (μg m^{-3})	9.2	2.5	3.1	3.1	3.7
	Difference (%)		-14		-8	
MAM	Mean (μg m^{-3})	12.6	12.4	16.2	9.0	9.5
	NMB (%)		-0.2	31.1		
	SD (μg m^{-3})	5.1	2.6	5.4	4.9	6.2
	Difference (%)		-31		-27	
JJA	Mean (μg m^{-3})	10.6	18.0	14.9	11.9	8.4
	NMB (%)		70.0	40.1		
	SD (μg m^{-3})	4.0	5.4	6.4	7.0	6.2
	Difference (%)		17		29	
SON	Mean (μg m^{-3})	11.0	10.7	13.2	12.3	11.3
	NMB (%)		-2.4	22.0		
	SD (μg m^{-3})	4.8	4.1	10.3	7.0	6.7
	Difference (%)		-23		8	

Atmos. Chem. Phys. Discuss., https://doi.org/10.5194/acp-2017-1074
Manuscript under review for journal Atmos. Chem. Phys.
Discussion started: 28 November 2017

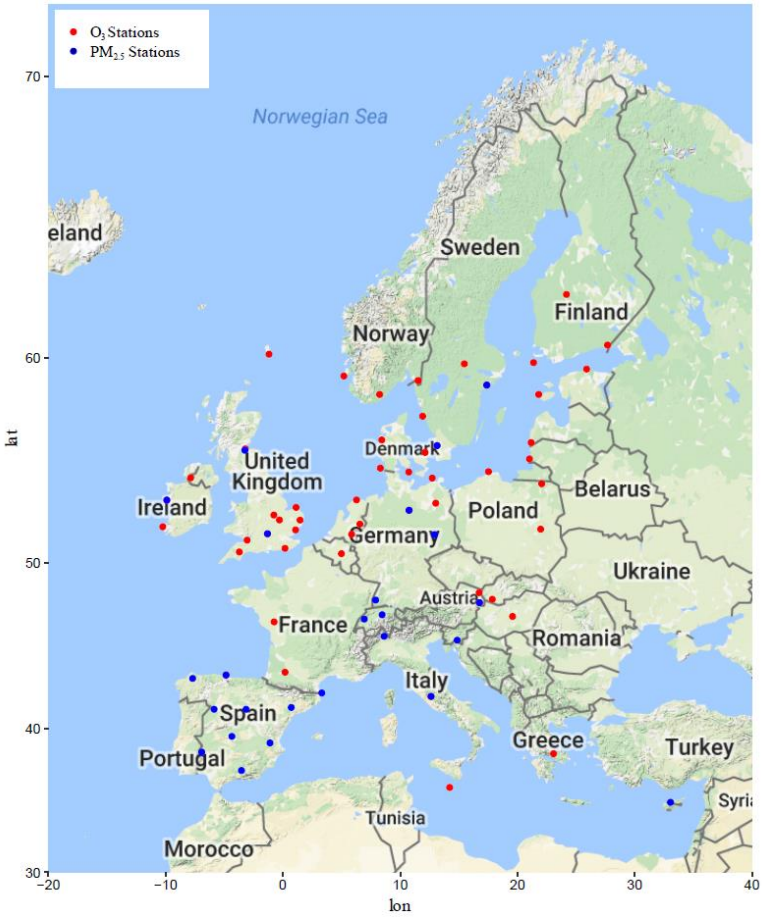

Figure 1: EMEP measurement stations with altitude less than or equal to 200 m, used for seasonal mean surface O_3 comparison to modelled concentrations (52 sites – red) and EMEP measurement stations used for seasonal mean $PM_{2.5}$ comparison to modelled concentrations (25 sites - blue)

Atmos. Chem. Phys. Discuss., https://doi.org/10.5194/acp-2017-1074
Manuscript under review for journal Atmos. Chem. Phys.
Discussion started: 28 November 2017

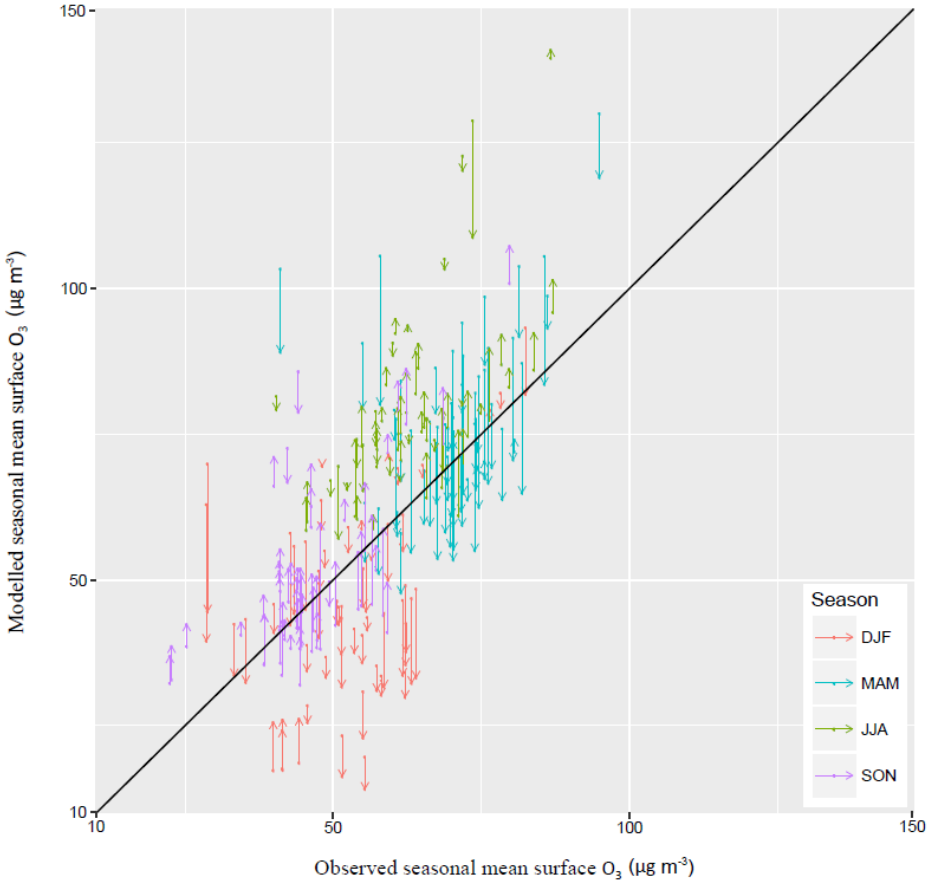

Figure 2: Seasonal mean modelled vs observed O_3 for 52 sites across the EMEP network for the year 2007. The arrow tails mark O_3 concentrations at the global resolution while the arrow heads represent the corresponding O_3 concentrations at the regional resolution. The 1:1 line shows agreement between observed and simulated O_3.

700

Atmos. Chem. Phys. Discuss., https://doi.org/10.5194/acp-2017-1074
Manuscript under review for journal Atmos. Chem. Phys.
Discussion started: 28 November 2017

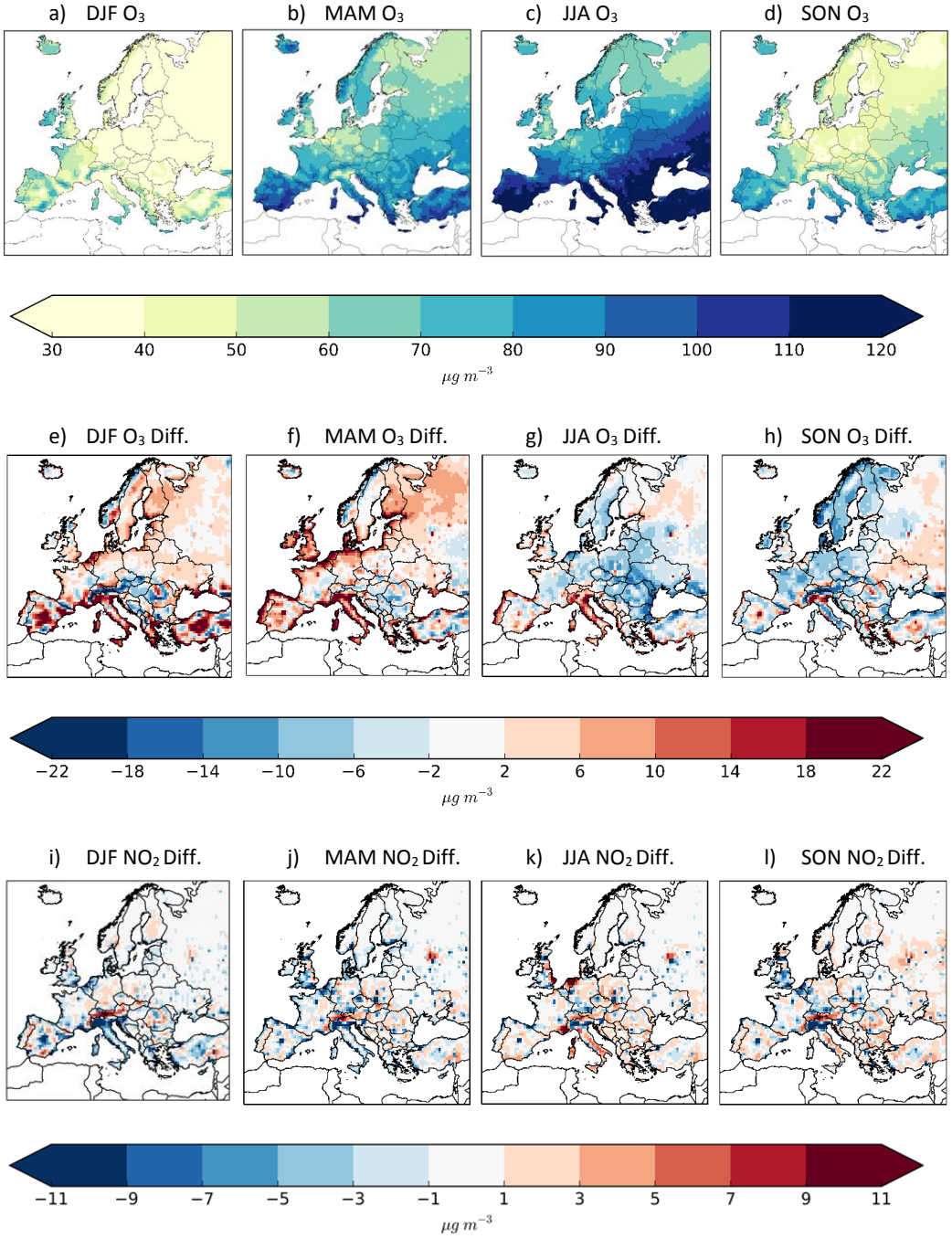

Figure 3: Seasonal mean O_3 simulated at the regional resolution (top panel), differences in seasonal mean O_3 between the global and regional resolutions ($O_{3\ \text{global resolution}} - O_{3\ \text{regional resolution}}$) (middle panel) and NO_2 ($NO_{2\ \text{global resolution}} - NO_{2\ \text{regional resolution}}$) (bottom panel). Blue regions in middle and bottom panels indicate that pollutant concentrations at the global resolution are lower (negative difference) while red regions indicate that concentrations are higher (positive difference) than those at the regional resolution.

Atmos. Chem. Phys. Discuss., https://doi.org/10.5194/acp-2017-1074
Manuscript under review for journal Atmos. Chem. Phys.
Discussion started: 28 November 2017

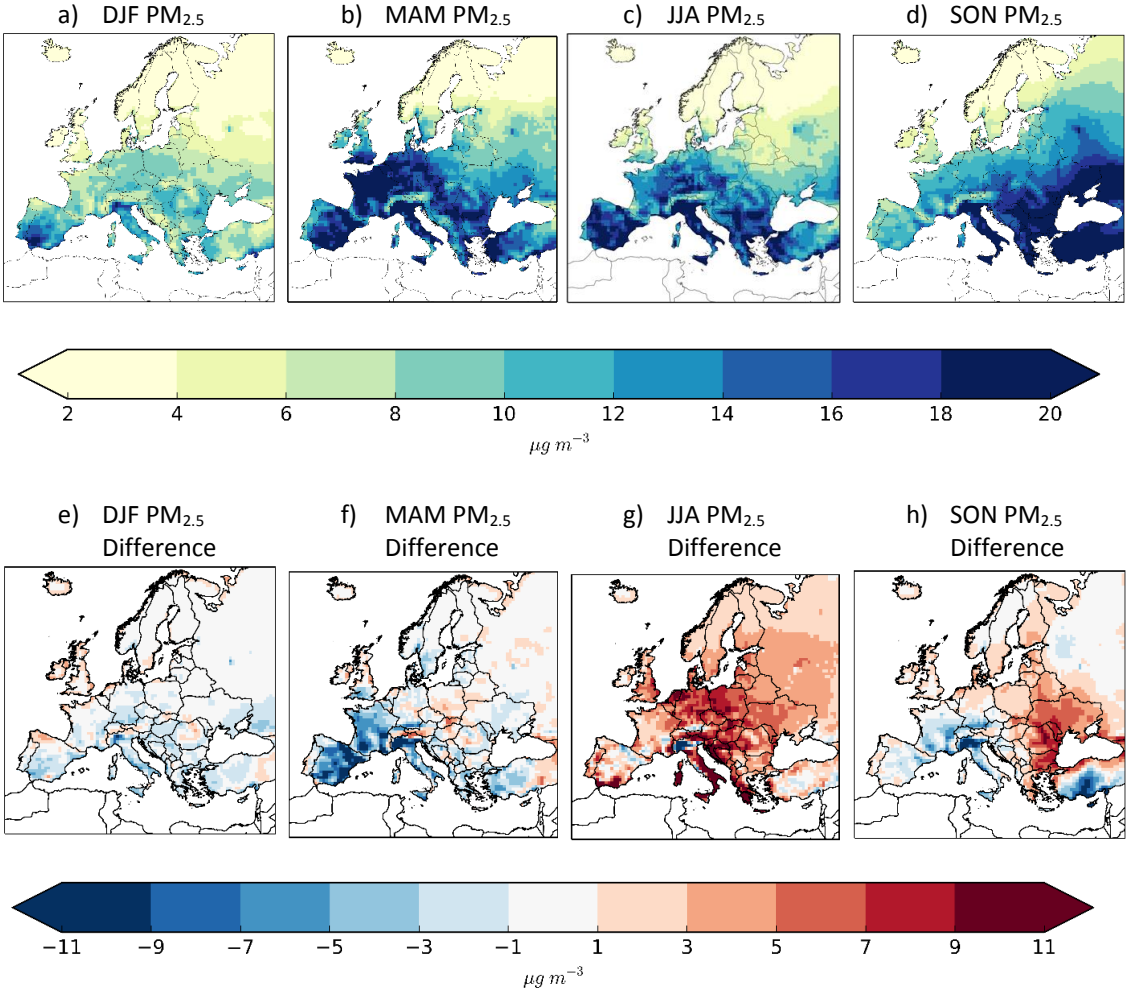

740 **Figure 4: Seasonal mean $PM_{2.5}$ simulate at the regional resolution (top panel) and differences between seasonal mean $PM_{2.5}$ at the global and regional resolution in 2007 ($PM_{2.5\ global\ resolution} - PM_{2.5\ regional\ resolution}$) (bottom panel).**

Atmos. Chem. Phys. Discuss., https://doi.org/10.5194/acp-2017-1074
Manuscript under review for journal Atmos. Chem. Phys.
Discussion started: 28 November 2017

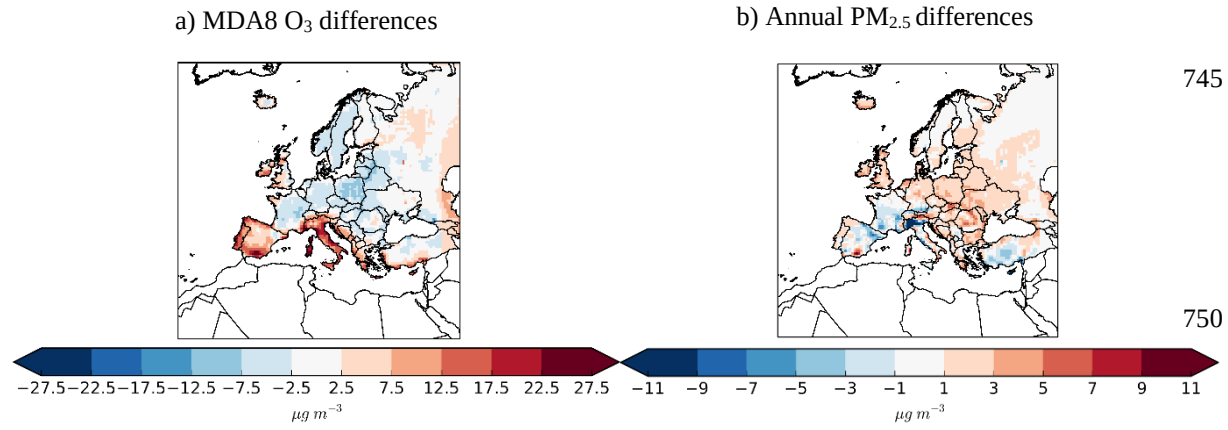

Figure 5: Differences in a) warm season (April-September) mean of daily maximum 8-hour running mean O_3 (concentrations above 70 µg m^{-3}) and b) annual mean $PM_{2.5}$ between the global and regional resolution (global – regional).

Atmos. Chem. Phys. Discuss., https://doi.org/10.5194/acp-2017-1074
Manuscript under review for journal Atmos. Chem. Phys.
Discussion started: 28 November 2017

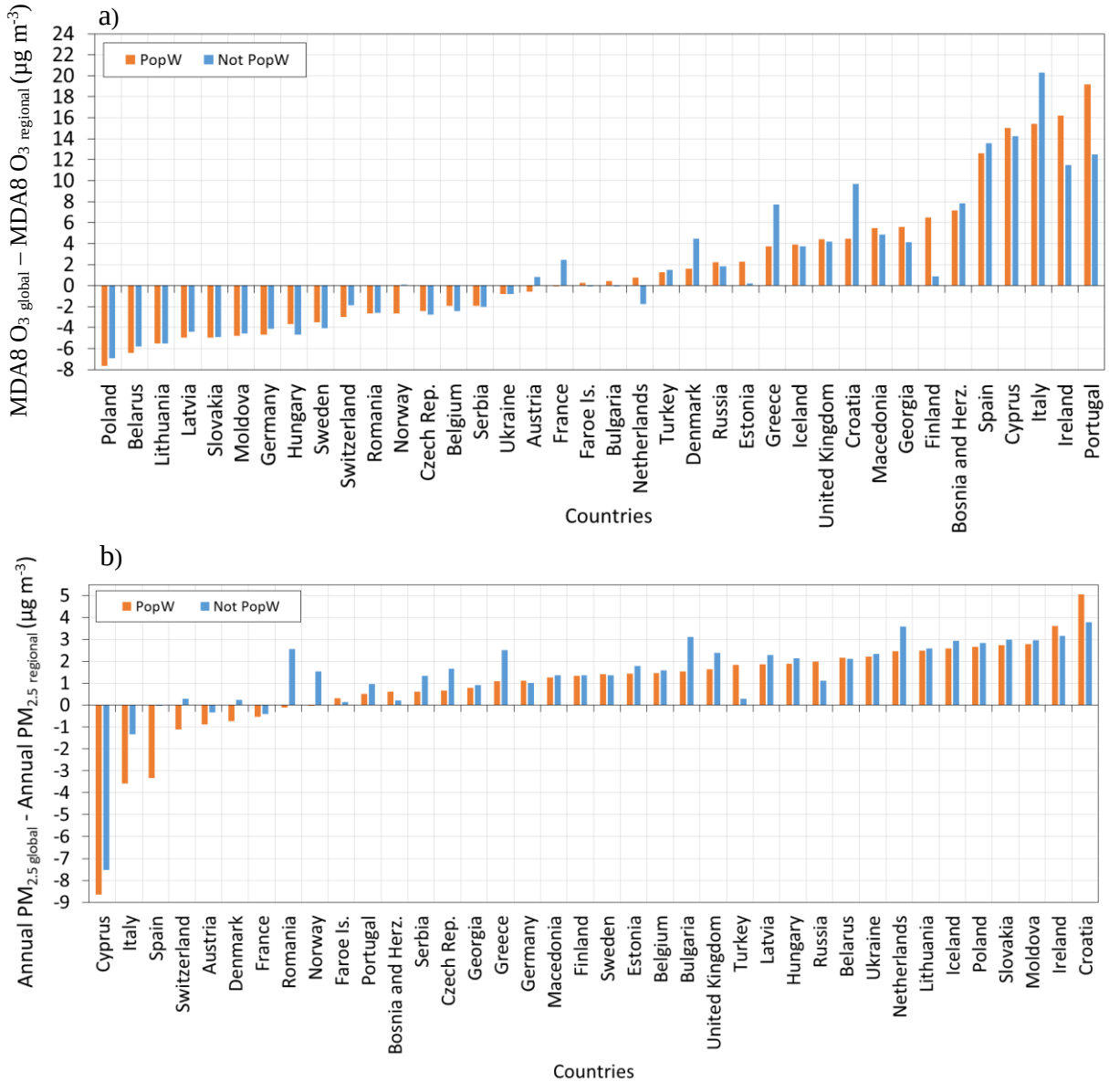

Figure 6: a) Differences between warm season mean daily maximum 8-hour running mean (MDA8) O_3 concentrations simulated at the two resolutions (global – regional) for population-weighted (PopW) concentrations (orange bars) and concentrations with no population-weighting (blue bars) b) same holds for annual mean $PM_{2.5}$ concentrations. Countries are ordered by differences in PopW pollutant concentrations between the two resolutions.

Atmos. Chem. Phys. Discuss., https://doi.org/10.5194/acp-2017-1074
Manuscript under review for journal Atmos. Chem. Phys.
Discussion started: 28 November 2017

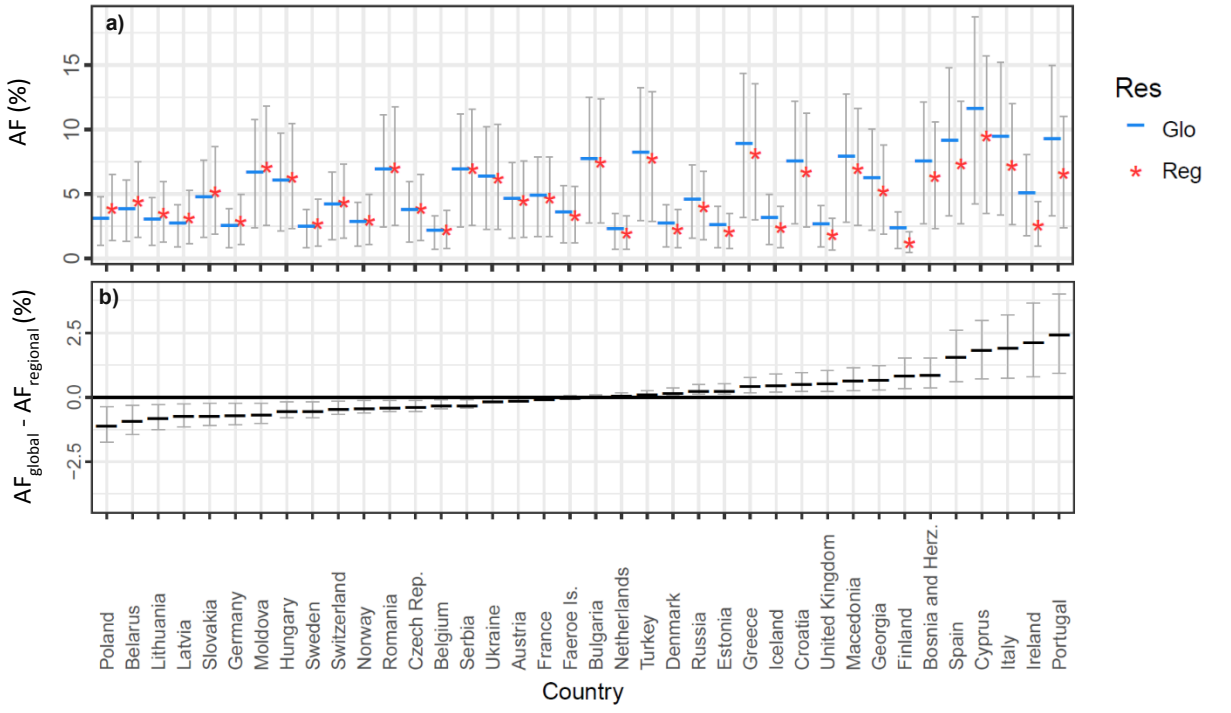

Figure 7: a) AF associated with long term exposure to daily maximum 8-hour running mean O_3 for each model resolution expressed as a percentage b) Differences in AF between the two resolutions expressed as a percentage for each European country ($AF_{global} - AF_{regional}$). Grey lines show the 95% C.I. which represents uncertainties associated only with the concentration-response coefficient used.

Atmos. Chem. Phys. Discuss., https://doi.org/10.5194/acp-2017-1074
Manuscript under review for journal Atmos. Chem. Phys.
Discussion started: 28 November 2017

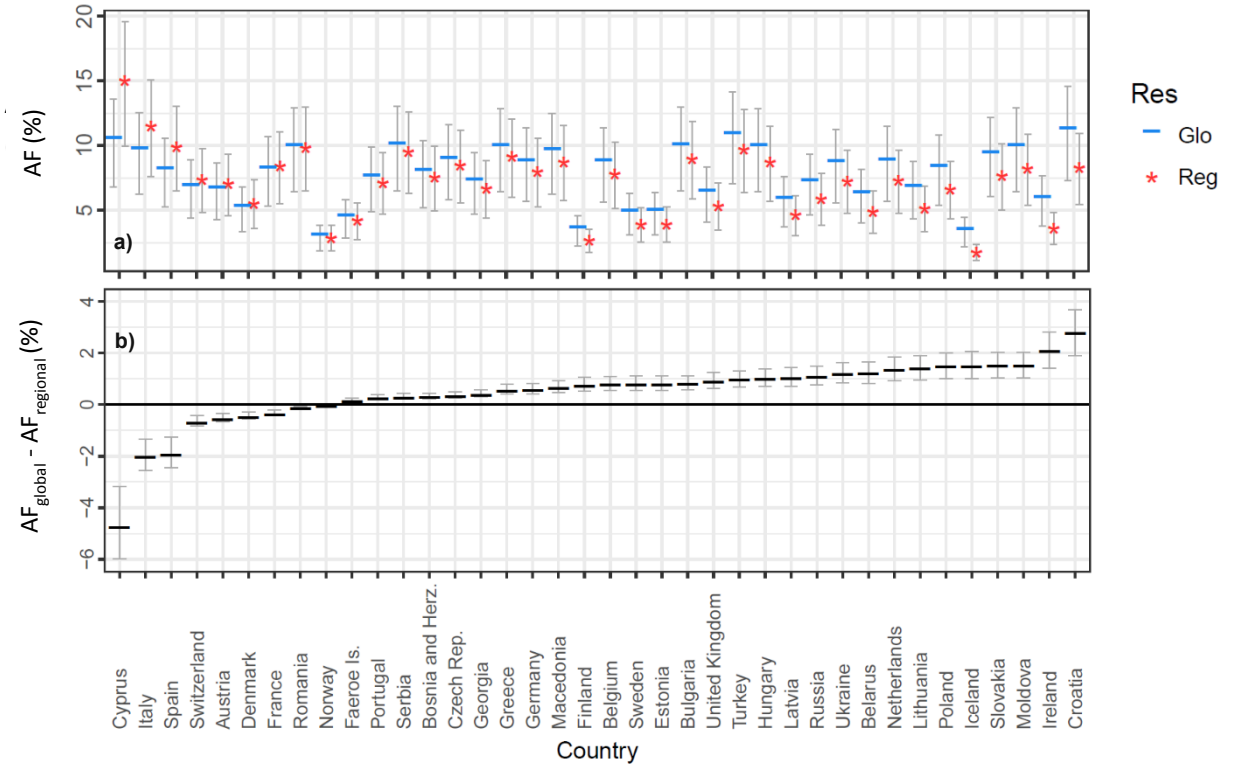

Figure 8: a) AF associated with long-term exposure to $PM_{2.5}$ for each model resolution expressed as a percentage b) Differences in AF between the two resolutions expressed as a percentage for each European country ($AF_{global} - AF_{regional}$). Grey lines show the 95 % C.I. which represents uncertainties associated only with the concentration-response coefficient used.